Journal of Applied Fluid Mechanics, Vol. 10, No. 5, pp. 1247-1260, 2017.
Available online at www.jafmonline.net, ISSN 1735-3572, EISSN 1735-3645.
DOI: 10.18869/acadpub.jafm.73.242.26842

Numerical Study of Flow Past Two Transversely Oscillating Triangular Cylinders in Tandem at Low Reynolds Number

Q. Zhai[1], H. K. Wang[1] and G. L. Yu[2†]

[1]*College of Harbour, Coastal and Offshore Engineering, Hohai University, Nanjing, Jiangsu, 210098, China*
[2]*School of Naval Architecture, Ocean and Civil Engineering, Shanghai Jiao Tong University, Shanghai, 200240, China*

†*Corresponding Author Email: yugl@sjtu.edu.cn*

(Received June 29, 2016; accepted April 20, 2017)

ABSTRACT

Flow past two tandem triangular cylinders forced to oscillate transversely in a uniform flow, is numerically investigated at a Reynolds number Re = 100. The incompressible Navier-Stokes equations in Arbitrary-Lagrangian-Eulerian formulation are solved by four-step fractional finite element method. The two cylinders are oscillated in phase and their motions are limited to low amplitudes with a wide frequency range. This study focuses on two typical spacings between the two cylinders, corresponding to vortex suppression (VS) regime and vortex formation (VF) regime respectively for flow past two stationary cylinders. Numerical results show that the response characteristics of two cylinders are significantly affected by the spacing, oscillation amplitude and frequency. For the VS spacing, both cylinders have a wider lock-on region, especially at relatively larger amplitude and higher frequency; the downstream wake patterns are mainly 2S and a combination of 2S* and 2S. However, for the VF spacing, the lock-on frequency range of the cylinders is even slightly narrower than that of a single oscillating cylinder; the wake field is more complex since it may comprises 2S, P+S and 2S* structures at some higher frequencies. Additionally, the hydrodynamic forces are also discussed in terms of mean and root mean square quantities, and reveal large differences between oscillating and stationary cylinders.

Keywords: Two triangular cylinders; Forced oscillation; Response characteristics; Wake pattern; Hydrodynamic Force.

NOMENCLATURE

A	oscillation amplitude
C_D	drag coefficient
C_L	lift coefficient
D	characteristic length
F_D	drag force acting on the cylinder
F_L	lift force acting on the cylinder
f_e	excitation frequency
f_o	natural vortex shedding frequency for flow past a stationary triangular cylinder
L	center-to-center spacing between two tandem triangular cylinders
p	fluid pressure
Re	Reynolds number
St	Strouhal number
t	time
u_i	fluid velocity in the ith direction
U_∞	free-stream velocity
w_i	mesh velocity in the ith direction
ν	kinematic viscosity of the fluid
ρ	fluid density

1. INTRODUCTION

Flow around bluff bodies has been a subject of extensive research during the past few decades, due to its significance in engineering applications such as skyscrapers, suspension bridges, heat exchangers, and offshore risers, etc. Regarding the fundamental physics of the flow, the periodic vortex shedding from the bodies would induce fluctuating forces which, in turn, may cause structural vibrations and damages. Thus, to avoid fatigue of structures and improve their performance, an in-depth investigation of interactions between flow and cylinder-like structures is very important.

Previous studies have greatly enhanced our understanding of flow past a single cylinder both numerically and experimentally (Luo *et al*. 1994; Williamson 1996; Zdravkovich 1997; Williamson and Govardhan 2004; Alonso *et al*. 2009; Yoon *et al*. 2010; Bao *et al*. 2011; Nemes *et al*. 2012). As confirmed in these works, some parameters, such as material properties of the cylinder, cross-section shape, flow incidence angle, and Reynolds number, can lead to significant changes in flow field, as well as flow-induced forces and vibrations of the cylinder.

Compared with a circular cylinder, the non-circular counterpart, such as square and triangular, has its own characteristic since the flow separation points are fixed at sharp corners of the non-circular section. Extensive studies have been performed on flow past a stationary triangular cylinder in the past decade. De and Dalal (2006) performed a numerical study of laminar flow over a triangular cylinder with varying low Reynolds numbers. A large-eddy simulation (LES) for flow over a triangular cylinder was reported by Camarri *et al*. (2006). Iungo and Buresti (2009) investigated the effects of cross-section shape and wind direction on a triangular cylinder in a wind-tunnel at high Reynolds number. Bao *et al*. (2010) considered flow over an equilateral triangular cylinder with different incidence angles at low Reynolds number range. Johansson *et al*. (2010) studied the vortex shedding past triangular cylinders using a *k-ε* model of turbulence. Wei *et al*. (2016) developed an hybrid RANS/LES model to simulate the complex turbulent flow around a triangular cylinder. Ng *et al*. (2016) performed a direct numerical simulation on the wake dynamics behind triangular cylinder at critical Reynolds numbers using a spectral-element method. Yagmur *et al*. (2017) investigated the flow characteristics around a triangle via PIV and LES methods. In addition, some studies focused on the heat transfer characteristics of a triangular cylinder placed in a channel with confined flows (De and Dalal 2006; Srikanth *et al*. 2010; Ali *et al*. 2011). Further experimental and numerical results are available for flow past an oscillating triangular cylinder (Alonso and Meseguer 2006; Alonso *et al*. 2007; Srigrarom and Koh 2008; Alonso *et al*. 2012; Alawadhi 2013). Srigrarom and Koh (2008) presented the self-excited rotational oscillation on isolated triangular cylinder. Alonso *et al*. (2012) investigated the transverse galloping of different triangular cross-sections though wind tunnel experiments. The numerical simulation of flow past a vertical oscillating triangular cylinder was accomplished by Alawadhi (2013) and, more recently, Wang *et al*. (2015) studied the flow-induced vibration of a triangular cylinder with different incidence angles at low Reynolds number.

On the other hand, flow interference between multiple cylinders are more frequently encountered in practical engineering, which further increases the complexity of the problem. Numerous studies focused on the classical case of flow past two stationary circular cylinders with various arrangements (Meneghini *et al*. 2001; Kang 2003; Sharman *et al*. 2005; Papaioannou 2006; Carmo *et al*. 2008; Mussa *et al*. 2009; Sumner 2010). Additionally, the free vibrations (Prasanth and Mittal 2009; Assi *et al*. 2010; Huera-Huarte and Gharib 2011; Carmo *et al*. 2013; Cui *et al*. 2014) and forced vibrations (Mahir and Rockwell 1996; Papaioannou *et al*. 2006; Yang and Zheng 2010; Bao *et al*. 2012; Bao *et al*. 2013; Yang *et al*. 2014) involving two circular cylinders have also been investigated extensively. It was found that the arrangement type and gap spacing have great influences upon the flow dynamics of two-cylinder system. However, to date, there are few studies on flow past two triangular cylinders. Wang *et al*. (2011) presented the self-excited rotational oscillation of two tandem triangular cylinders, and identified three different states of motion of the system with the increase of spacing. Ghafouri *et al*. (2015) studied the deposition and dispersion of aerosols over two tandem triangular cylinders.

The current work aims to numerically investigate the flow past two transversely oscillating triangular cylinders in tandem, which has not been done yet so far. But to start with, the problems of flow past two stationary triangles and a single oscillating triangle are simulated as the reference cases. Then, the effects of cylinder spacing, oscillation amplitude and frequency on the flow characteristics of two oscillating triangular cylinders are investigated.

2. NUMERICAL METHOD

2.1 Fractional Step Algorithm

The incompressible fluid flow is governed by the Navier-Stokes equations, which can be expressed in the non-dimensional form:

$$\frac{\partial u_i}{\partial t}+u_j u_{i,j}=-\frac{\partial p}{\partial x}+\frac{1}{\mathrm{Re}}\frac{\partial^2 \tau_{ij}}{\partial x_j \partial x_j} \tag{1}$$

$$u_{i,i}=0 \tag{2}$$

wherein the Reynolds number Re is defined as Re = $U_\infty D/\nu$. The stress tensor τ_{ij} is written as:

$$\tau_{ij}=\frac{\partial u_i}{\partial x_j}+\frac{\partial u_j}{\partial x_i} \tag{3}$$

In the present study, the Navier-Stokes equations are solved by using the semi-implicit four-step fractional method (Wang *et al*. 2015), which can be carried out as follows:

$$\frac{\hat{u}_i-u_i^n}{\Delta t}+u_j^n \hat{u}_{i,j}=\frac{1}{2\,\mathrm{Re}}\left[\left(u_{i,j}^n+u_{j,i}^n\right)_{,j}+\left(\hat{u}_{i,j}+\hat{u}_{j,i}\right)_{,j}\right] -p_{,i}^n-f_i \tag{4}$$

$$\frac{u_i^*-\hat{u}_i}{\Delta t}=p_{,i}^n \tag{5}$$

$$p_{,jj}^{n+1}=\frac{1}{\Delta t}u_{i,i}^* \tag{6}$$

$$\frac{u_i^{n+1}-u_i^*}{\Delta t}=-p_{,i}^{n+1} \tag{7}$$

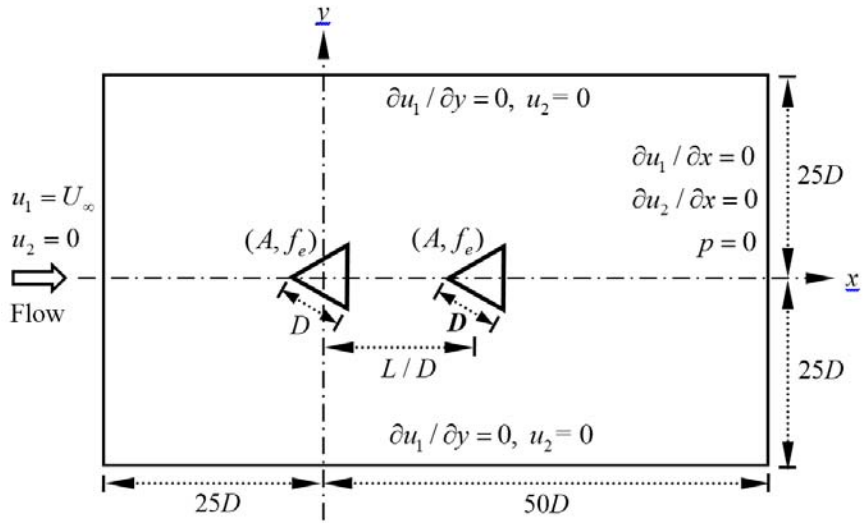

Fig. 1. Two tandem triangular cylinders forced to oscillate transversely to the flow: schematic of the computational domain and boundary conditions.

Table 1 Comparison of numerical results for flow past a stationary triangular cylinder at Re = 100

Studies	$C_{D,\,mean}$	$C_{L,\,rms}$	St
De and Dalal (2006)	1.7607	0.2968	0.1966
Alawadhi (2013)	1.757	-	0.18204
The present	1.710	0.285	0.196

The solution procedure based on the fractional step algorithm can be described here as: (i) solve Eqs. (4)-(5) to get the intermediate velocities $\hat{u}_i$ and u_i^*; (ii) obtain the pressure p from Eq. (6); (iii) correct the velocity field by solving Eq. (7).

2.2 Mesh Motion Scheme

To account for the cylinder motion in the flow field, the fractional step algorithm is extended to the arbitrary Lagrangian-Eulerian (ALE) formulation of the Navier-Stokes equations (Donea 1982; Hughes and Tezduyar 1984). The ALE formulation can be implemented by substituting the convective velocity in Eq. (1) with $c_j = u_j - w_j$, where c_j is the relative velocity between the fluid and the mesh. For the purpose of mesh movement, a modified Laplacian method, presented by Masud *et al*. (2007) is incorporated into the ALE scheme.

3. PROBLEM DESCRIPTION

The flow configuration and boundary conditions are illustrated in Fig. 1. Two transversely oscillating triangular cylinders in tandem, each of side length D, are placed in a computational domain defined as $\Omega = [-25D, 50D] \times [-25D, 25D]$. The origin of the Cartesian coordinates is located at the center of the upstream cylinder. The inlet boundary has uniform flow velocity of $u_1 = U_\infty$ and $u_2 = 0$, while at the outlet, the flow conditions are $\partial u_i / \partial x = 0$ and $p = 0$. Symmetric conditions are applied on the lateral boundaries: $\partial u_1 / \partial y = 0$ and $u_2 = 0$. The no-slip condition is imposed upon the cylinder surface. The transverse oscillations of two cylinders are governed by $Y(t) = A \sin(2\pi f_e t)$. Numerical simulations are conducted at two different amplitudes, $A/D = 0.1$ and 0.25, with varying frequency ratio in a range of $0.5 \le f_e/f_o \le 2.0$ at Re = 100. The center-to-center spacing between the cylinders takes two values: $L/D = 2.0$ and 5.0, corresponding to two distinct flow patterns observed in the stationary two-cylinder system.

Some important flow parameters used in this study, such as drag coefficient C_D, lift coefficient C_L, and strouhal number St, are also defined as follows:

$$C_D = \frac{2F_D}{\rho U_\infty^2 D}, \quad C_L = \frac{2F_L}{\rho U_\infty^2 D}, \quad \mathrm{St} = \frac{f_o D}{U_\infty} \tag{8}$$

4. NUMERICAL VALIDATION AND REFINEMENT

The developed finite element code based on the four-step fractional method has been validated in our previous work (Wang *et al*. 2015). In this section, the accuracy of the numerical model is further demonstrated by applying it for flow past a stationary triangular cylinder at Re = 100. Table 1 compares the present results with those in other literature, involving the mean drag coefficient $C_{D,mean}$, the root mean square of lift coefficient $C_{L,rms}$, and the Strouhal number St. Excellent

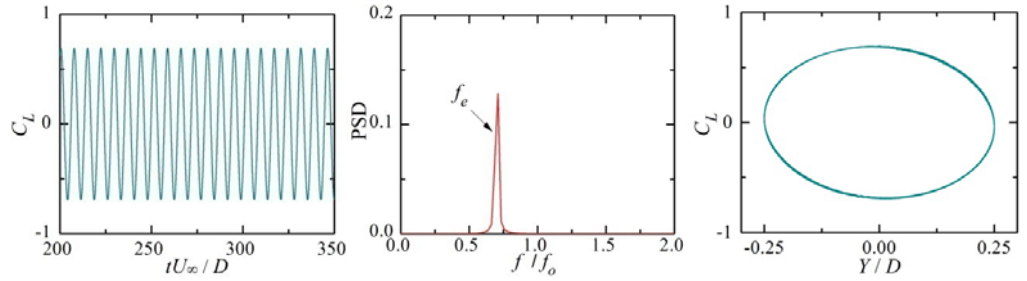

(a) $(A/D, f_e/f_o) = (0.25, 0.7)$

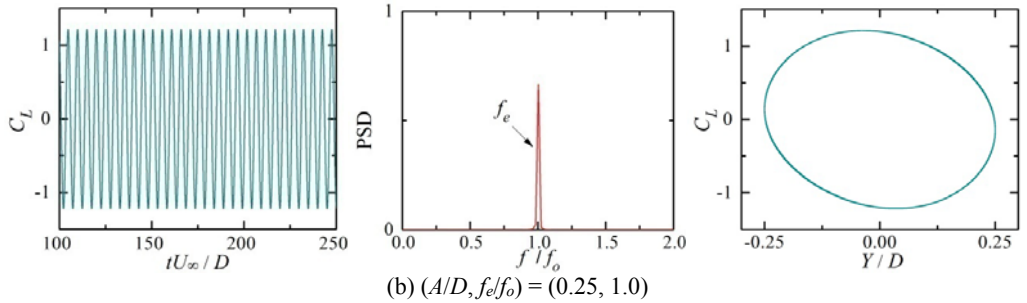

(b) $(A/D, f_e/f_o) = (0.25, 1.0)$

Fig. 2. Time evolutions of the lift coefficient C_L (left column), power spectral density (PSD) of the lift coefficient (middle column) and phase portraits for the oscillating cylinder at: (a) $(A/D, f_e/f_o) = (0.25, 0.7)$; (b) $(A/D, f_e/f_o) = (0.25, 1.0)$.

agreement is obtained between our numerical results and the published data.

5. RESULTS AND DISCUSSIONS

5.1 Flow Past a Single Oscillating Triangular Cylinder

Alawadhi (2013) has numerically investigated the influence of oscillation frequency and amplitude on the drag and lift forces acting on a triangular cylinder. In this section, the main intention is to determine the lock-on state of a single triangular cylinder, where the vortex shedding frequency is completely dominated by the excitation frequency f_e rather than the natural vortex shedding frequency f_o. The calculations are run for two oscillation amplitudes A/D = 0.1 and 0.25 at Re = 100. The frequency ratio is varied in the range of $0.0 \le f_e/f_o \le 2.0$, expecting to cross the lock-on region. The single triangular cylinder is forced to oscillate also as $Y(t) = A \sin(2\pi f_e t)$.

Fig. 2 illustrates the lock-on states for two cases of $(A/D, f_e/f_o)$ = (0.25, 0.7) and (0.25, 1.0). As observed in the left column, the time evolutions of the lift coefficient are absolutely periodic and characterized by a pure sinusoidal response. The PSD (power spectral density) of the lift coefficient shown in the middle column highlights the sinusoidal response and clearly presents that the dominant frequency is f_e. Phase portraits in the right column exhibit a single limit cycle, which is consistent with the perfect sinusoidal response.

The two cases of $(A/D, f_e/f_o)$ = (0.25, 0.6) and (0.25, 1.5) are selected to illustrate the unlock-on responses, as shown in Fig. 3. Time evolutions of the lift coefficient (left column) are no longer purely sinusoidal, but exhibit a beating behavior. The power spectra of the lift (middle column) shows two peaks (one significant peak at f_e, the other small peak at f_o or at a modulation frequency f_m). Instead of a single cycle, multiple cycles are observed in the phase portraits (right column) since the lift signal contains more than one frequency.

Fig. 4 shows the vorticity fields when the cylinder moves to the top position ($Y = A$) at A/D = 0.25. For the lock-on state (Figs. 4(a) and (b)), the vortex shedding pattern is commonly called 2S mode (Williamson and Roshko 1988), in which two single vortices are shed per circle. In the far wake at f_e/f_o = 1.0, the positive and negative vortices form two parallel rows, which is the 2S* pattern previously mentioned (Yang and Zheng 2010). For the unlock-on state (Figs. 4(c) and (d)), the wake is shown to be disordered, due to the multiple frequency components in the cylinder oscillation. Moreover, an asymmetric P+S pattern (Williamson and Roshko 1988) is observed at a higher excitation frequency (f_e/f_o = 1.5, see Fig. 4(d)), where a pair of vortices and a single vortex are shed per cycle.

Fig. 5 shows the simulation results for an oscillating triangular cylinder with different spacings, amplitudes and frequencies at Re = 100, along with the results for an oscillating circular cylinder (Bao *et al*. 2012) and square cylinder (Singh *et al*. 2009) at the same Re for the sake of comparison. The schematic of the lock-on and unlock-on regions is illustrated in Fig. 5(a). In general, the lock-on

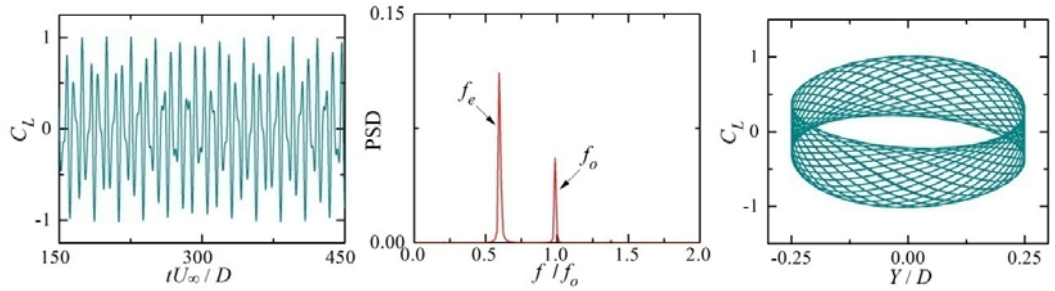

(a) (A/D, f_e/f_o) = (0.25, 0.6)

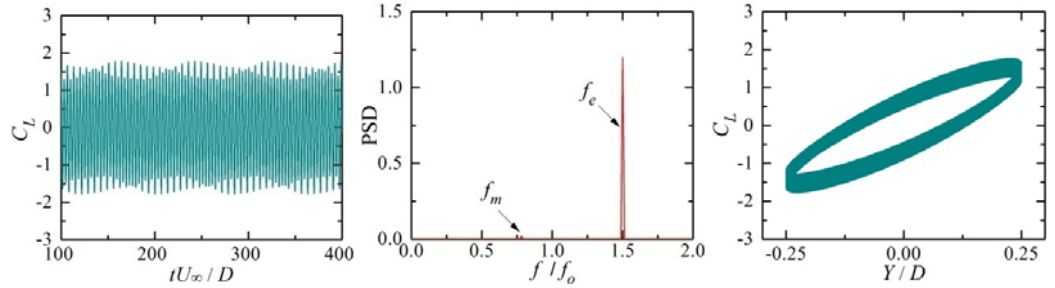

(b) (A/D, f_e/f_o) = (0.25, 1.5)

Fig. 3. Time evolutions of the lift coefficient C_L (left column), power spectral density (PSD) of the lift coefficient (middle column) and phase portraits for the oscillating cylinder at: (a) (A/D, f_e/f_o) = (0.25, 0.6); (b) (A/D, f_e/f_o) = (0.25, 1.5).

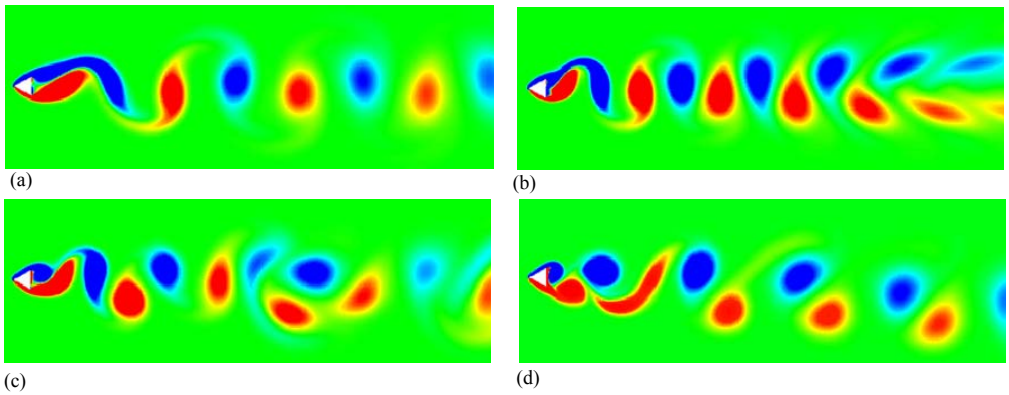

(a) (b) (c) (d)

Fig. 4. Instantaneous vorticity fields for the flow past an oscillating triangular cylinder at different excitation frequencies: (a) (A/D, f_e/f_o) = (0.25, 0.7); (b) (A/D, f_e/f_o) = (0.25, 1.0); (c) (A/D, f_e/f_o) = (0.25, 0.6); and (d) (A/D, f_e/f_o) = (0.25, 1.5).

regions for these cylinders are broadened with the increase of the oscillation amplitude. The lock-on region for the triangular cylinder is found within the frequency range of $0.82 \le f_e/f_o \le 1.02$ at A/D = 0.1, but expands to $0.7 \le f_e/f_o \le 1.04$ at A/D = 0.25. Compared with the cases of the circular and square cylinders, both left and right boundaries of the lock-on region for the triangular cylinder shift towards lower frequency; meanwhile, the bandwidth becomes slightly larger. Figs. 5(b)-(d) show the variations of the force coefficients with the excitation frequency. As observed in Figs. 5(b) and (c), for the triangular cylinder, the curves of $C_{D,mean}$ or $C_{D,rms}$ are globally similar to those of the circular and square cylinders at a comparable amplitude, with a dominant peak around the end of the lock-on region. However, the values of drag force for the triangular cylinder are significantly larger than those for the circular cylinder over the examined frequency range. As shown in Fig. 5(d), near the end of the lock-on region, the $C_{L,rms}$ curves of triangular and square cylinders show a small drop, while the lift of circular cylinder exhibits a continuous increase. Despite such differences, all $C_{L,rms}$ curves of these cylinders rise rapidly beyond the lock-on region, which can be explained by reason that high-frequency oscillation leads to large pressure differences between the upper and lower surfaces of the cylinders and thus large variation in the lift coefficient.

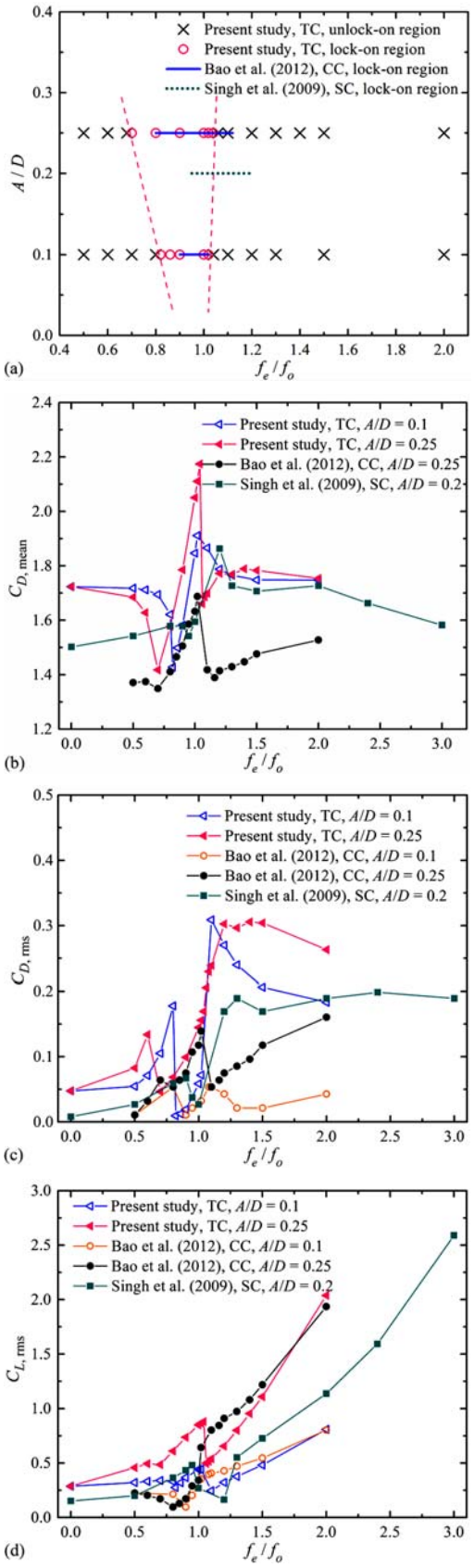

Fig. 5. Simulation results for flow past an oscillating cylinder: (a) Strouhal number; (b) mean drag coefficient; (c) root mean square of drag coefficient; (d) root mean square of lift coefficient. TC: triangular cylinder; CC: circular cylinder; SC: square cylinder.

5.2 Flow Past Two Oscillating Triangular Cylinders in Tandem

As mentioned previously, the oscillations of a single cylinder can be categorized into two major responses of lock-on and unlock-on, depending on whether the vortex shedding frequency is dominated by the excitation frequency. Through further careful observation, the unlock-on state of two oscillating cylinders in this study is subdivided into two subclasses: transitional and quasi-periodic modes, the same modes also used by Papaioannou *et al*. (2006) and Yang *et al*. (2010). The identification of these modes is mainly based on the examination of (i) the phase portrait of lift force versus transverse displacement and (ii) the power spectra of lift force. In transitional mode, the power spectra of lift force is controlled by peaks at the excitation frequency, but some other small peaks may just emerge resulting in a small modulation in the phase portrait, thus deviating from the tight limit circle obtained from the lock-on response. In quasi-periodic mode, the power spectra of lift force shows multiple peaks at different frequencies; consequently, the phase portrait for this mode exhibits a highly irregular pattern.

Flow past two cylinders under forced oscillation display more complex responses. Fig. 6 illustrates the schematic of the response states for two oscillating triangular cylinders with respect to different combinations of spacing, amplitude, and frequency. At the VS spacing, since the flow oscillations are closely coupled between the upstream and downstream zones, the flow is lock-on within a wide frequency range (Yang and Zheng 2010). As can be seen from Fig. 6(a), at different amplitudes (A/D = 0.1 and 0.25) for the VS spacing (L/D = 2.0), the lock-on region of the upstream cylinder is substantially broadened compared to the single cylinder case, especially toward higher frequency. Similar results are observed for the downstream cylinder at higher amplitude (Fig. 6b). Furthermore, with the increase of the excitation frequency for a fixed amplitude, the lock-on state of two cylinders first occurs in the vicinity of natural frequency for two stationary cylinders ($f_e/f_{oo} \approx 1.0$), which is corresponding to $f_e/f_o \approx 0.740$ (Here, f_{oo} and f_o are 0.145 and 0.196 respectively), then switches to the transitional or quasi-periodic modes. Subsequently, the oscillation response returns to the lock-on state again at higher frequency, due to the intensified couple effect. Such phenomenon were previously observed in the experiments by Mahir and Rockwell (1996), who showed that the lock-on state can exist intermittently when two tandem circular cylinders are oscillating in-phase at small spacing. In addition, Papaioannou *et al*. (2006) provided numerical evidence revealing the existence of "holes" that represent the unlock-on state may appear inside lock-on regions for two oscillating circular cylinders.

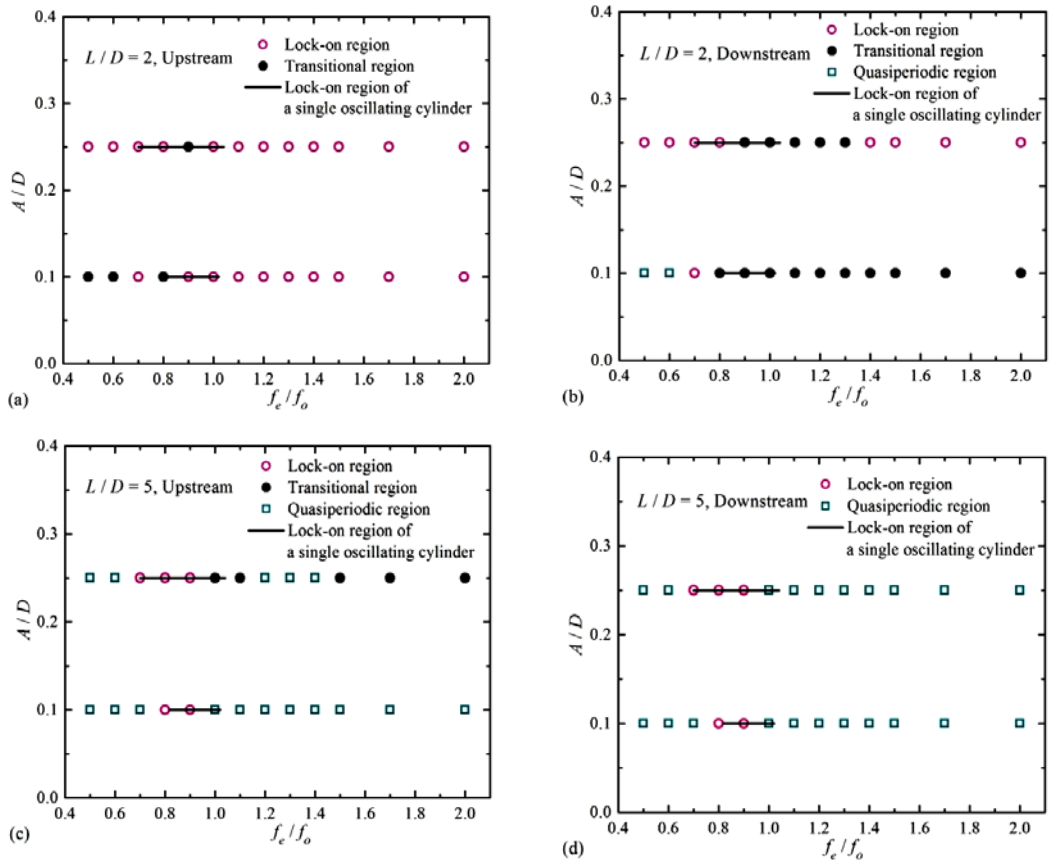

Fig. 6. Schematic of the lock-on/unlock-on regions for two oscillating triangular cylinders in tandem with different spacings, amplitudes and frequencies.

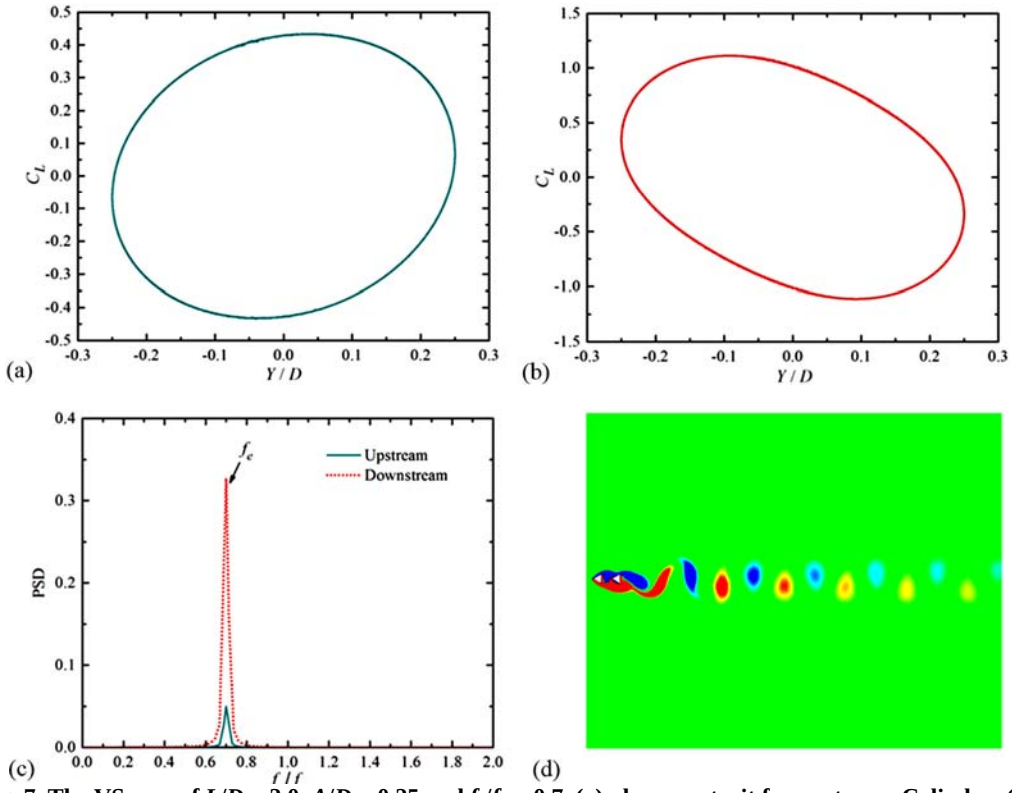

Fig. 7. The VS case of L/D = 2.0, A/D = 0.25 and f_e/f_o = 0.7. (a) phase portrait for upstream Cylinder; (b) phase portrait for downstream Cylinder; (c) lift power spectra for two Cylinders; and (d) vorticity contour plot.

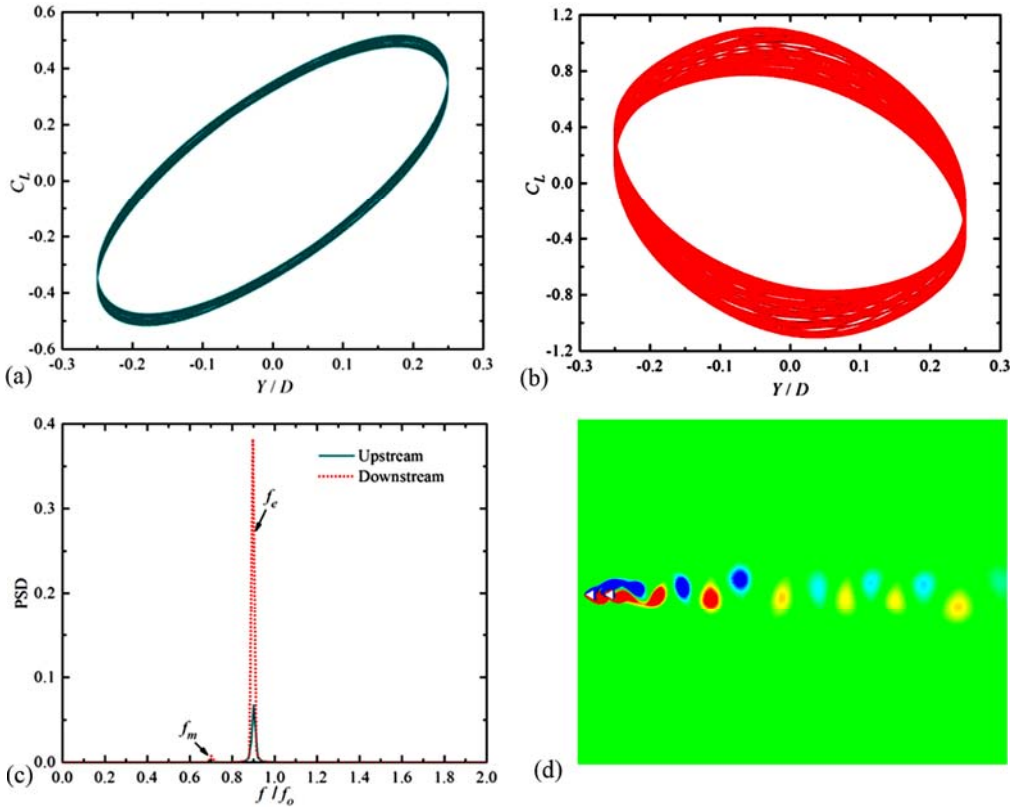

Fig. 8. The VS case of *L*/*D* = 2.0, *A*/*D* = 0.25 and f_e/f_o = 0.9. (a) phase portrait for upstream Cylinder; (b) phase portrait for downstream Cylinder; (c) lift power spectra for two Cylinders; and (d) vorticity contour plot.

In the VS case with A/D = 0.25 and f_e/f_o =0.9, the phase portraits of two cylinders become a transational mode instead of a single closed orbit (Figs. 8(a) and (b)). The power spectra shows only one peak at f_e for the upstream cylinder, but two peaks (one significant peak at f_e, the other small peak at f_m) for the downstream cylinder (Fig. 8(c)). The downstream near wake starts to show a P+S pattern, then develops into a 2S pattern in the far wake (Fig. 8(d)).

For the VS spacing and A/D = 0.25, further increase of the excitation frequency to f_e/f_o = 1.5 takes the oscillations of both cylinders back to the lock-on state, as shown in Fig. 9. In this case, the near wake displays a 2S* pattern, while the far wake changes into a 2S pattern.

As can be seen from Figs. 6(c) and (d), unlike the VS case, the lock-on state of two oscillating cylinders at the VF spacing (L/D = 5.0) only occurs in the narrower region in the vicinity of natural frequency for the stationary counterpart ($f_e/f_{oo} \approx 1.0$, f_{oo} =0.179), corresponding to $f_e/f_o \approx 0.913$. When f_e/f_o exceeds 1.0, the vortex shedding cannot be entrained by the excitation frequency, resulting in the unlock-on state. Therefore, at this spacing, the oscillation system shows more sensitive to change from lock-on to other states, which is similar to the case of a single oscillating cylinder. It is worth noting that both upstream and downstream cylinders always exhibit the lock-on state simultaneously, which is a quite different situation to that of the VS case. This can be attributed to the complete synchronization between vortices shedding from the two cylinders and flow impingement on the downstream cylinder.

Fig. 10 shows the lock-on state of two cylinders for the VF spacing at A/D = 0.25 and f_e/f_o =0.8. The phase portraits and power spectra of the lift behave similarly to those in the VS lock-on state, as shown in Figs. 10(a)-(c) and Figs. 9(a)-(c). The vorticity contours in Fig. 10(d) displays a clear 2S* vortex shedding pattern over the downstream wake.

The unlock-on case at A/D = 0.25 and f_e/f_o = 1.5 for the VF spacing is shown in Fig. 11. The phase portraits indicate that the upstream and downstream cylinders are in different response modes: the former is transitional but the latter quasi-periodic (Figs. 11(a) and (b)). The power spectra of lift force shows that only one significant peak appears at f_e for upstream cylinder, while two major peaks coexist at f_e and f_m for downstream cylinder (Fig. 11(c)). In the near wake of downstream cylinder, the 2S pattern persists, but the far wake changes into P+S and 2S* structures (Fig. 11(d)).

For the VF spacing at A/D = 0.1 and f_e/f_o = 1.5 in Fig. 12, the phase portraits of both cylinders display a quasi-periodic mode (Figs. 12(a) and (b)); two significant peaks in the power spectra of the lift appear at f_o and f_m for each cylinder (Fig. 12(c)); the downstream near wake has a combination of 2S* and P+S, developing into a 2S pattern in the far wake (Fig. 12(d)).

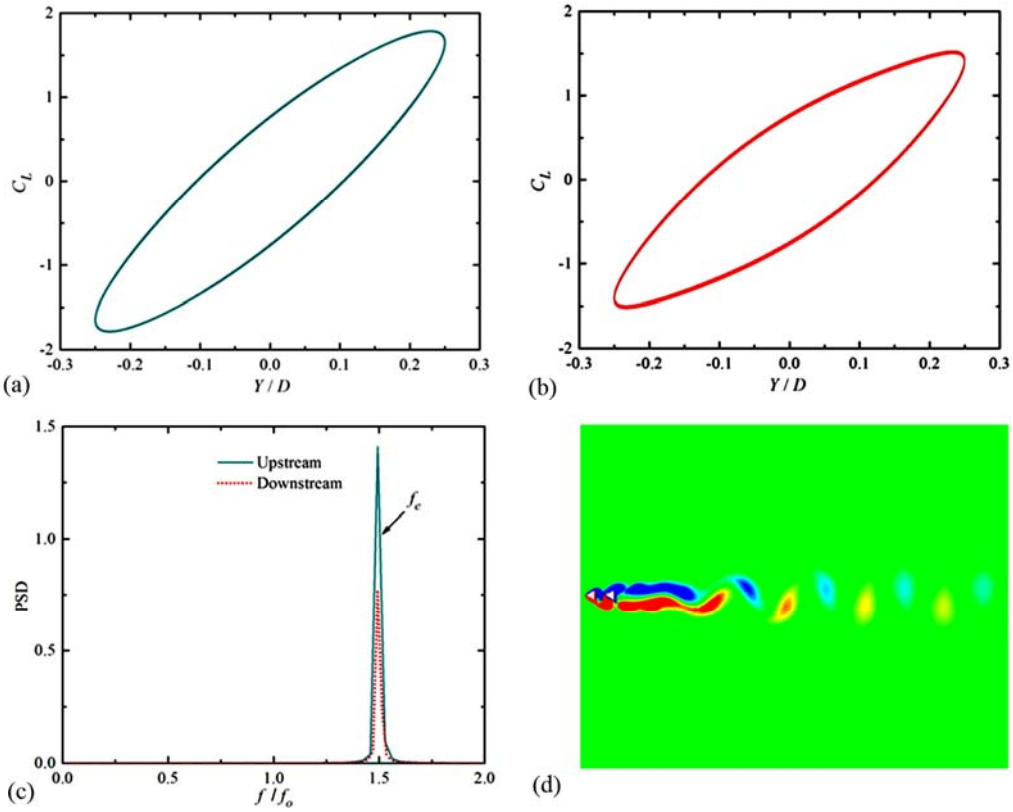

Fig. 9. The VS case of L/D = 2.0, A/D = 0.25 and f_e/f_o = 1.5. (a) phase portrait for upstream Cylinder; (b) phase portrait for downstream Cylinder; (c) lift power spectra for two Cylinders; and (d) vorticity contour plot.

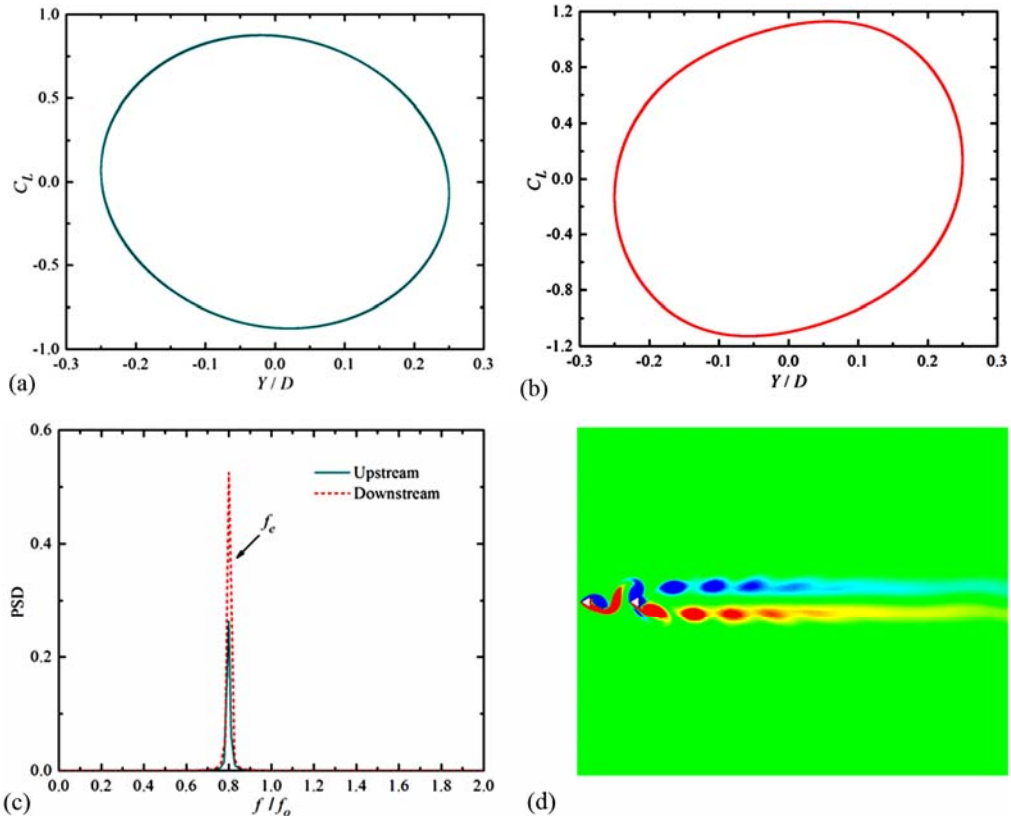

Fig. 10. The VS case of L/D = 5.0, A/D = 0.25 and f_e/f_o = 0.8. (a) phase portrait for upstream Cylinder; (b) phase portrait for downstream Cylinder; (c) lift power spectra for two Cylinders; and (d) vorticity contour plot.

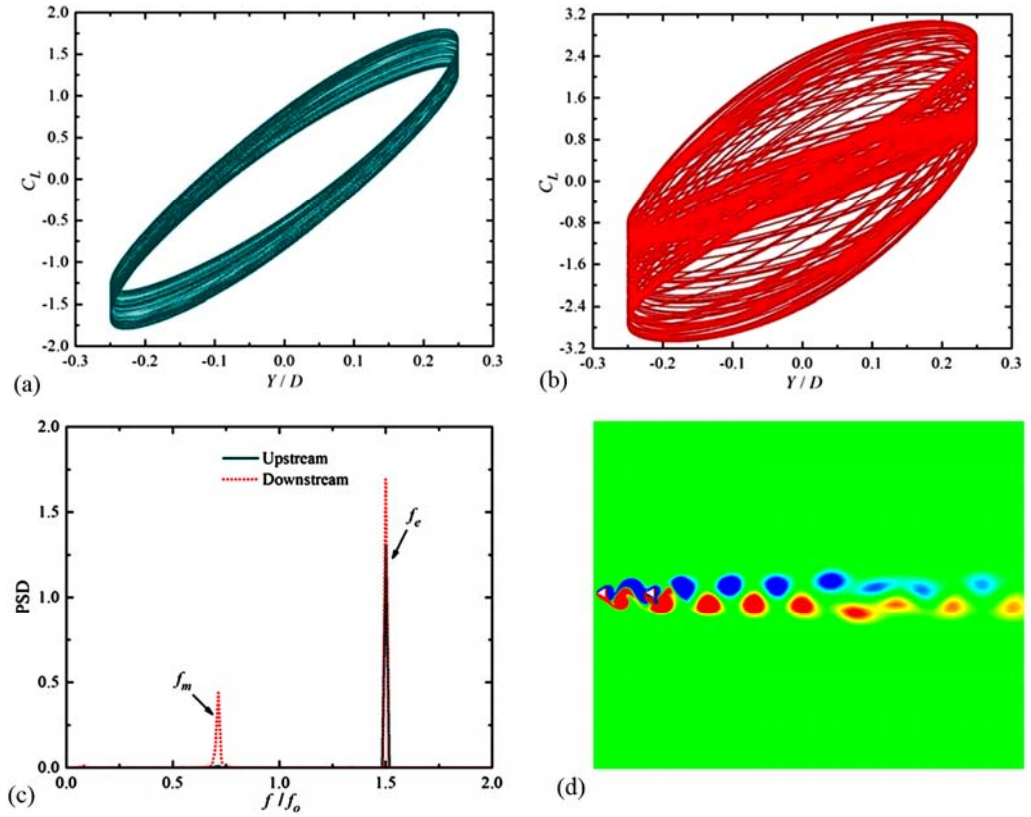

Fig. 11. The VS case of L/D = 5.0, A/D = 0.25 and f_e/f_o = 1.5. (a) phase portrait for upstream Cylinder; (b) phase portrait for downstream Cylinder; (c) lift power spectra for two Cylinders; and (d) vorticity contour plot.

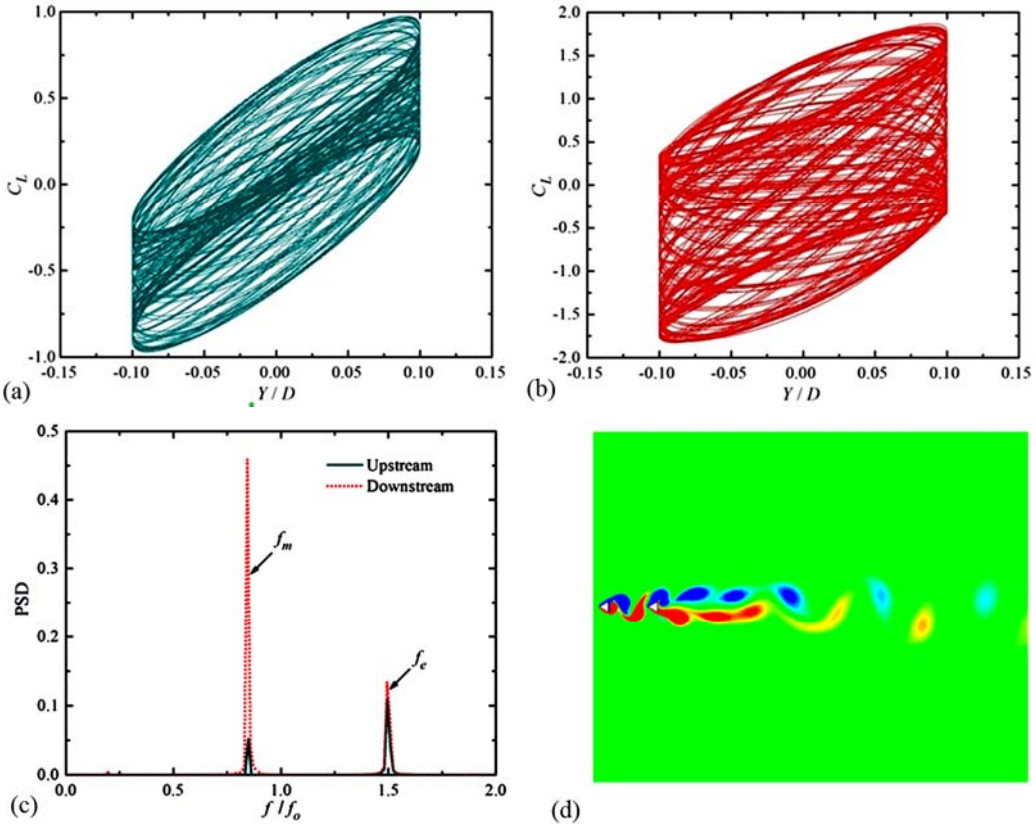

Fig. 12. The VS case of L/D = 5.0, A/D = 0.1 and f_e/f_o = 1.5. (a) phase portrait for upstream Cylinder; (b) phase portrait for downstream Cylinder; (c) lift power spectra for two Cylinders; and (d) vorticity contour plot.

Table 2 Vortex shedding patterns of two oscillating triangular cylinders in tandem

f_e / f_o	$L/D = 2$		$L/D = 5$	
	$A/D = 0.1$	$A/D = 0.25$	$A/D = 0.1$	$A/D = 0.25$
0.5	2S	2S	2S*, 2S	2S*, 2S
0.6	2S	2S	2S*, 2S	2S
0.7	2S	2S	2S*, 2S	2S*
0.8	2S	2S, 2S*	2S*	2S*
0.9	2S*, 2S	S+P, 2S	2S*	2S*
1.0	2S*, 2S	S+P, 2S	2S*, 2S	2S*, 2S
1.1	2S*, 2S	S+P, 2S	2S*, 2S	2S, 2S*
1.2	2S*, 2S	S+P, 2S	S+P, 2S	2S, P+S, 2S*
1.3	2S*, 2S	S+P, 2S	S+P, 2S	2S, 2S*
1.4	2S*, 2S	2S*, 2S	2S*, P+S, 2S	2S, 2S*
1.5	2S*, 2S	2S*, 2S	2S*, P+S, 2S	2S, P+S, 2S*
1.7	2S*, 2S	2S*, 2S	2S*, 2S	2S, 2S*
2.0	2S*, 2S	2S*, 2S	2S*, 2S	2S, 2S*

A summary of the vortex shedding patterns for all examined cases is presented in Table 2. As can be seen from the table, for the VS spacing ($L/D = 2.0$), the downstream wake is mostly a 2S pattern at lower frequency, while it becomes a combination of 2S* and 2S patterns at higher frequency. However, these wake patterns cannot be used to identify the lock-on and unlock-on states. For the VF spacing ($L/D = 5.0$), the wake flow is more complex since it may comprises 2S, P+S and 2S* patterns at some high frequencies. Note that the pure 2S* pattern only occurs in the lock-on cases at this spacing.

The drag and lift coefficients of the two oscillating triangular cylinders are illustrated in Fig. 13. For comparison, the results of the stationary counterpart are also given in the figure. It can be seen that in most cases for the VS spacing, the $C_{D,mean}$ and $C_{L,rms}$ of the two oscillating cylinders are larger than those of the stationary counterpart, with highter oscillation amplitudes producing higher values. For the upstream cylinder, the $C_{D1,mean}$ at $A/D = 0.1$ is nearly constant over the examined frequency, and it is approximately equal to the value of the stationary cylinder (Fig. 13(a)). This means that the excitation frequency has little influence on $C_{D1,mean}$ at small amplitude for the VS spacing. The curves of $C_{L1,rms}$ at $A/D = 0.1$ and 0.25 exhibits a monotonous increase with the increase in the excitation frequency (Fig. 13(b)). For the downstream cylinder, both $C_{D2,mean}$ and $C_{L2,rms}$ obtain a peak within the lower frequency region of lock-on state (Figs. 13(c) and (d)). At higher frequency, the $C_{L2,rms}$ continues to increase and reaches its maximum.

For the VF spacing, the curves of $C_{D1,mean}$ and $C_{L1,rms}$ of the upstream cylinder behave similarly to those observed for a single oscillating cylinder (see Figs. 13(a) and (b), Figs. 5(b) and (d)), indicative of the diminished effect of the downstream cylinder. However, because the vortices shed from the upstream cylinder impinge on the windward sides of the downstream cylinder, the $C_{D2,mean}$ exhibits more irregular fluctuations around the value of the stationary counterpart (Fig. 13(c)).

6. CONCLUSIONS

In this paper, numerical simulations of flow past two tandem triangular cylinders subjected to transverse oscillation of in-phase mode are performed at low Reynolds number of Re = 100. The oscillations of two cylinders are dominated by harmonic motion with low amplitudes of $A/D = 0.1$ and 0.25, and varying frequency in the range of $0.5 \leq f_e/f_o \leq 2.0$. The investigations on the cylinder response are conducted for two typical spacings: $L/D = 2.0$ and 5.0. The results of flow past two stationary tandem triangles and a single oscillating triangle are also presented for comparison. Main findings can be summarized as follows:

For the VS spacing of $L/D = 2.0$, the lock-on frequency range for the upstream oscillating cylinder is substantially widen at different amplitudes ($A/D = 0.1$, 0.25), compared with that for a single oscillating cylinder. Similar results are also observed for the downstream oscillating cylinder, but the wake degrades its lock-on state at relatively smaller amplitude of $A/D = 0.1$. Additionally, a hole represents the unlock-on state may exist within the lock-on regions of the cylinders. The vorticity contours show that the wake patterns are mainly 2S at lower frequency, and a combination of 2S* and 2S at higher frequency. However, the wake patterns cannot be used to distinguish the response state.

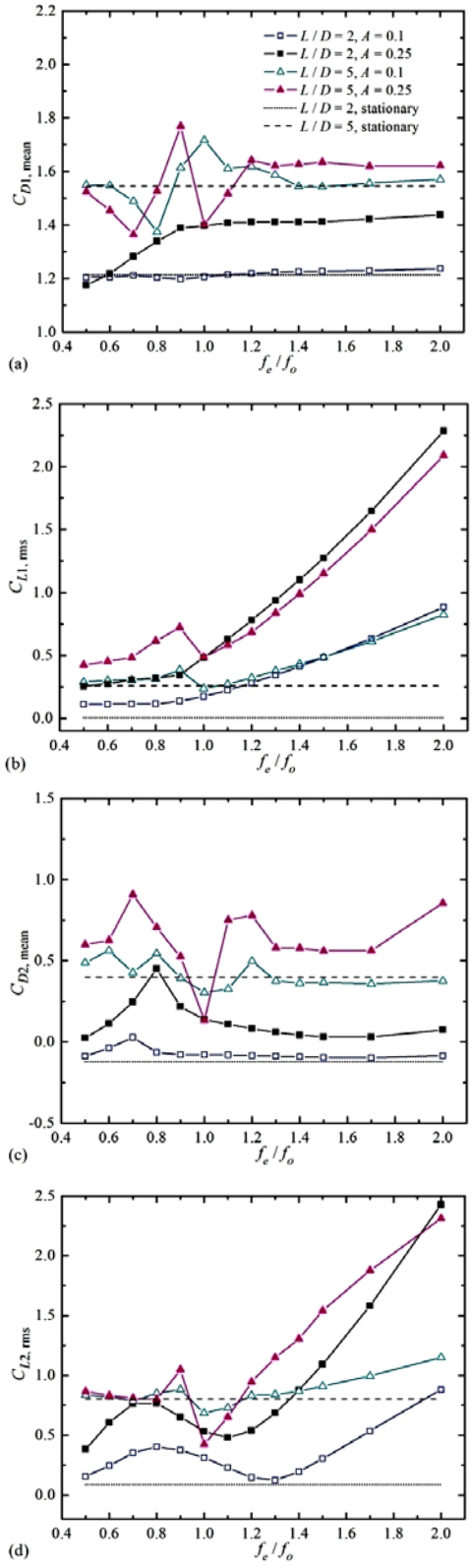

Fig. 13. Variations of the force coefficients for two oscillating triangular cylinders in tandem with different spacings, amplitudes and frequencies. Left column: mean drag coefficient ((a) upstream cylinder, (c) downstream cylinder); Right column: root mean square of lift coefficient ((b) upstream cylinder, (d) downstream cylinder).

For the VF spacing of L/D = 5.0, the two tandem cylinders have the same lock-on regions, but with the width being slightly narrower than that for a single cylinder. The wake flow, on the other hand, is more complex and may contains 2S, 2S*, and P+S patterns at some higher frequencies. It is found that the lock-on response is always accompanied by a pure 2S* vortex shedding pattern at this spacing.

The drag and lift forces of both oscillating and stationary triangular cylinders are also investigated. In most cases for the VS spacing, the hydrodynamic forces of two oscillating cylinders exceed those of the stationary counterpart, with larger oscillation amplitudes producing larger values. For the VF spacing, the drag and lift forces acting on the upstream oscillating cylinder behave similarly to those on a single oscillating cylinder, with a peak appearing in the lock-on region; however, the flow impingment induces more complex changes in hydrodynamic forces on the downstream oscillating cylinder.

ACKNOWLEDGEMENTS

This work is financially supported by the Natural Science Foundation of Jiangsu Province (Grant No.BK20160865, No.BK20160870), and the National Natural Science Foundation of China (Grant No.51609077).

REFERENCES

Alawadhi, E. M. (2013). Numerical simulation of fluid flow past an oscillating triangular cylinder in a channel. *Journal of Fluids Engineering* 135(4), 041202.

Ali, M., O. Zeitoun and A. Nuhait (2011). Forced convection heat transfer over horizontal triangular cylinder in cross flow. *International Journal of Thermal Sciences* 50(1), 106-114.

Alonso, G. and J. Meseguer (2006). A parametric study of the galloping stability of two-dimensional triangular cross-section bodies. *Journal of Wind Engineering and Industrial Aerodynamics* 94(4), 241-253.

Alonso, G., A. Sanz-Lobera and J. Meseguer (2012). Hysteresis phenomena in transverse galloping of triangular cross-section bodies. *Journal of Fluids and Structures* 33(33), 243-251.

Alonso, G., E. Valero and J. Meseguer (2009). An analysis on the dependence on cross section geometry of galloping stability of two-dimensional bodies having either biconvex or rhomboidal cross sections. *European Journal of Mechanics-B/Fluid* 28(2), 328-334.

Alonso, G., J. Meseguer and I. Pérez-Grande (2007). Galloping stability of triangular cross-sectional bodies: A systematic approach. *Journal of Wind Engineering and Industrial Aerodynamics* 95(9-11), 928-940.

Assi, G. R. S., P. W. Bearman and J. R. Meneghini (2010). On the wake-induced vibration of tandem circular cylinders: the vortex interaction excitation mechanism. *Journal of Fluid Mechanics* 661(4), 365-401.

Bao, S., S. Chen, Z. Liu, J. Li, H. Wang and C. Zheng (2012). Simulation of the flow around an upstream transversely oscillating cylinder and a stationary cylinder in tandem. *Physics of Fluids* 24(2), 023603.

Bao, Y., D. Zhou, C. Huang, Q. Wu and X. Chen (2011). Numerical prediction of aerodynamic characteristics of prismatic cylinder by finite element method with Spalart-Allmaras turbulence model. *Computers and Structures* 89(3-4), 325-338.

Bao, Y., D. Zhou and J. Tu (2013). Flow characteristics of two in-phase oscillating cylinders in side-by-side arrangement. *Computers and Fluids* 71(1), 124-145.

Bao, Y., D. Zhou and Y. J. Zhao (2010). A two-step Taylor-characteristic-based Galerkin method for incompressible flows and its application to flow over triangular cylinder with different incidence angles. *International Journal for Numerical Methods in Fluids* 62(11), 1181-1208.

Camarri, S., M. V. Salvetti and G. Buresti (2006). Large-eddy simulation of the flow around a triangular prism with moderate aspect-ratio. *Journal of Wind Engineering and Industrial Aerodynamics* 94(5), 309-322.

Carmo, B. S., G. R. S. Assi and J. R. Meneghini (2013). Computational simulation of the flow-induced vibration of a circular cylinder subjected to wake interference. *Journal of Fluids and Structures* 41(8), 99-108.

Carmo, B. S., S. J. Sherwin, P. W. Bearman and H. J. Willden (2008). Wake transition in the flow around two circular cylinders in staggered arrangements. *Journal of Fluid Mechanics* 597(3), 1-29.

Cui, Z., M. Zhao and B. Teng (2014). Vortex-induced vibration of two elastically coupled cylinders in side-by-side arrangement. *Journal of Fluids and Structures* 44(7), 270-291.

De, A. K. and A. Dalal (2006). Numerical simulation of unconfined flow past a triangular cylinder. *International Journal for Numerical Methods in Fluids* 52(7), 801-821.

De, A. K. and A. Dalal (2007). Numerical study of laminar forced convection fluid flow and heat transfer from a triangular cylinder placed in a channel. *Journal of Heat Transfer* 129(5), 646-656.

Donea, J., S. Giuliani and J. P. Halleux (1982). An arbitrary Lagrangian-Eulerian finite element method for transient dynamic fluid-structure interactions. *Computer Methods in Applied Mechanics and Engineering* 33(1-3), 689-723.

Ghafouri, S., M. Alizadeh, S. M. Seyyedi, H. H. Afrouzi and D. D. Ganji (2015). Deposition and dispersion of aerosols over triangular cylinders in a two-dimensional channel; effect of cylinder location and arrangement. *Journal of Molecular Liquids* 206(8), 228-238.

Huera-Huarte, F. J. and M. Gharib (2011). Vortex- and wake-induced vibrations of a tandem arrangement of two flexible circular cylinders with far wake interference. *Journal of Fluids and Structures* 27(5-6), 824-828.

Hughes, T. J. R. and T. E. Tezduyar (1984). Finite element methods for first-order hyperbolic systems with particular emphasis on incompressible Euler equations. *Computer Methods in Applied Mechanics and Engineering* 45(1), 217-284.

Iungo, G. V. and G. Buresti (2009). Experimental investigation on the aerodynamic loads and wake flow features of low aspect-ratio triangular prisms at different wind directions. *Journal of Fluids and Structures* 25(7), 1119-1135.

Johansson, S. H., L. Davidson and E. Olsson (2010). Numerical simulation of vortex shedding past triangular cylinders at high Reynolds number using a *k-ε* turbulence model. *International Journal for Numerical Methods in Fluids* 16(10), 859-878.

Kang, S. (2003). Characteristics of flow over two circular cylinders in a side-by-side arrangement at low Reynolds numbers. *Physics of Fluids* 15(9), 2486-2498.

Luo, S. C., M. G. Yazdani, Y. T. Chew and T. S. Lee (1994). Effects of incidence and afterbody shape on flow past bluff cylinders. *Journal of Wind Engineering and Industrial Aerodynamics* 53(3), 375-399.

Mahir, N. and D. Rockwell (1996). Vortex formation from a forced system of two cylinders. Part □: tandem arrangement. *Journal of Fluids and Structures* 10(5), 473-489.

Mahir, N. and D. Rockwell (1996). Vortex formation from a forced system of two cylinders. Part □: side-by-side arrangement. *Journal of Fluids and Structures* 10(5), 491-500.

Masud, A., M. Bhanabhagvanwala and R. A. Khurram (2007). An adaptive mesh rezoning scheme for moving boundary flows and fluid-structure interaction. *Computers and Fluids* 36(1), 77-91.

Meneghini, J. R., F. Saltara, C. L. R. Siqueira and J. A. Ferrar (2001). Numerical simulation of flow interference between two circular cylinders in tandem and side-by-side arrangements. *Journal of Fluids and Structures* 15(2), 327-350.

Nemes, A., J. Zhao, D. L. Jacono and J. Sheridan (2012). The interaction between flow-induced

vibration mechanisms of a square cylinder with varying angles of attack. *Journal of Fluid Mechanics* 710(5), 102-130.

Ng, Z. Y., T. Vo, W. K. Hussam and G. J. Sheard (2016). Two-dimensional wake dynamics behind cylinders with triangular cross-section under incidence angle variation. *Journal of Fluids and Structures* 63, 302-324.

Papaioannou, G. V., D. K. P. Yue and M. S. Triantafyllou (2006). Evidence of holes in Arnold tongues of flow past two oscillating cylinders. *Physical Review Letters* 96(1), 014501.

Papaioannou, G. V., D. K. P. Yue, M. S. Triantafyllou and G. E. Karniadakis (2006). Three-dimensionality effects in flow around two tandem cylinders. *Journal of Fluid Mechanics* 558(7), 387-413.

Prasanth, T. K. and S. Mittal (2009). Vortex-induced vibration of two circular cylinders at low Reynolds number. *Journal of Fluids and Structures* 25(25), 731-741.

Singh, A. P., A. K. De, V. K. Carpenter, V. Eswaran and K. Muralidhar (2009). Flow past a transversely oscillating square cylinder in free stream at low Reynolds numbers. *International Journal for Numerical Methods in Fluids* 61(6), 658-682.

Srigrarom, S. and A. K. G. Koh (2008). Flow field of self-excited rotationally oscillating equilateral triangular cylinder. *Journal of Fluids and Structures* 24(5), 750-755.

Srikanth, S., A. K. Dhiman and S. Bijjam (2010). Confined flow and heat transfer across a triangular cylinder in a channel. *International Journal of Thermal Sciences* 49(11), 2191-2200.

Sumner, D. (2010). Two circular cylinders in cross-flow: a review. *Journal of Fluids and Structures* 26(6), 849-899.

Wang, H., D. Zhao, W. Yang and G. Yu (2015). Numerical investigation on flow-induced vibration of a triangular cylinder at a low Reynolds numbers. *Fluid Dynamics Research* 47(1), 015501.

Wang, S., L. Zhu, X. Zhang and G. He (2011). Flow past two freely rotatable triangular cylinders in tandem arrangement. *Journal of Fluids Engineering* 133(8), 081202.

Wei, Q., H. X. Chen and M. A. Zheng (2016). An hybrid RANS/LES model for simulation of complex turbulent flow. *Journal of Hydrodyna- mics*, *Ser.B* 28(5), 811-820.

Williamson, C. H. K. (1996). Vortex dynamics in the cylinder wake. *Annual Review of Fluid Mechanics* 28, 477-539.

Williamson, C. H. K. and A. Roshko (1988). Vortex formation in the wake of an oscillating cylinder. *Journal of Fluids and Structures* 2(4), 355-81.

Williamson, C. H. K. and R. Govardhan (2004). Vortex-induced vibrations. *Annual Review of Fluid Mechanics* 36(1), 413-455.

Yagmur, S., S. Dogan, M. H. Aksoy, I. Goktepeli and M. Ozgoren (2017). Comparison of flow characteristics around an equilateral triangular cylinder via PIV and Large Eddy Simulation methods. *Flow Measurement and Instrumen-tation*.

Yang, X. and Z. C. Zheng (2010). Nonlinear spacing and frequency effects of an oscillating cylinders in the wake of a stationary cylinder. *Physics of Fluids* 22(4), 043601.

Yang, Y., T. B. Aydin and A. Ekmekci (2014). Flow past tandem cylinders under forced vibration. *Journal of Fluids and Structures* 44(7), 292-309.

Yoon, D. H., K. S. Yang and C. B. Choi (2010). Flow past a square cylinder with an angle of incidence. *Physics of Fluids* 22(4), 043603.

Zdravkovich, M. M. (1997). Flow Around Circular Cylinders. New York: Oxford University Press.